Original Contributions

Mammalian Genome

Mammalian Genome 7, 2–5 (1996).

High-resolution genetic mapping of the hypodactyly (*Hd*) locus on mouse Chromosome 6

J.W. Innis,[1,2] K. Kazen-Gillespie,[1] L.C. Post,[1] J. McGorman[1]

[1]Department of Human Genetics, University of Michigan, Med. Sci. II, M4708, Ann Arbor, Michigan 48109-0618, USA
[2]Department of Pediatrics, University of Michigan, Med. Sci. II, M4708, Ann Arbor, Michigan 48109-0618, USA

Received: 8 June 1995 / Accepted: 4 August 1995

Hd is a semidominant mutation in mice that leads to failure of development of the first four digits on each foot and more proximal maldevelopment of the carpals, metacarpals, tarsals, and metatarsals in homozygous mutant animals (Hummel 1970). Heterozygous animals show absence or shortening of the first phalanx and/or terminal claw of the hallux on the hindfeet. Most homozygous mutant mice die in utero for unknown reasons; those that survive to adulthood are infertile. The defects within the autopod imply that the normal product of the *Hd* gene may be critical for the development of the digital arch.

The hypodactyly mutation arose spontaneously on the MYA strain and was outcrossed to a C57BL/6J (B6) mouse which carried the Va^J allele (N11) (Hummel 1970). The Va^J/+,*Hd*/+ offspring were crossed to B6 for one generation. Both mutations were subsequently crossed onto a [C57BL/6J × C3H/FeJ]F_1 (B6C3Fe) nonagouti hybrid to increase breeding efficiency. Affected heterozygotes were successively crossed to B6C3Fe hybrids for over 70 generations (Hope Sweet, personal comm.). Thus, present-day affected mice retain a very small region flanking the mutation similar to the original MYA strain. *Hd* was originally mapped within linkage group XI between obese (*ob*) and waved-1 (*wa1*) (Hummel, 1970). Subsequently, it was mapped near but recombinant with the *Hoxa* locus on Chr 6 (Mock et al. 1987). In the latter study, one crossover event was identified between *Hd* and *Hoxa3* (formerly *Hox-1.5;* see Scott 1992), placing *Hd* most likely proximal to *Hoxa3* at a genetic distance of 0.85 ± 0.85 cM.

To explore the mechanism of the malformation, we have undertaken a positional cloning strategy to determine the molecular basis of the *Hd* mutation. To accurately define the location of the mutation we have produced and typed a large intersubspecific backcross segregating *Hd.*

B6C3Fe-a/a-*Hd* Va^J mice were mated to CASA/Rk (an inbred strain of *M. m. castaneus*), and the *Hd* heterozygous F_1 females were backcrossed to CASA/Rk males. The *Hd* heterozygous F_1 males were crossed with B6 females. Phenotypic characterization of the backcross progeny mice (N2) was based on the appearance of the first digit on each hindfoot; 1383 N2 progeny were scored visibly for phenotype (*Hd*/+ or +/+). The heterozygous phenotype ranged from shortening of the nail on the hallux of both hindfeet to complete absence of the first digit. Phenotypic abnormalities were usually bilaterally symmetrical; 690 were *Hd*/+ (49.9%) and 693 were +/+ (50.1%). These data support the reported autosomal dominant mode of inheritance with complete penetrance for the mutation (Hummel 1970).

DNA was prepared from the spleen of N2 progeny by a salting out procedure (Miller et al. 1988). Oligonucleotide primers (obtained from Research Genetics) specific for polymorphic markers linked to a short region of mouse Chr 6 were used to amplify DNA from the backcross progeny. DNA typing was performed by staining PCR products after electrophoresis in 6% polyacrylamide with ethidium bromide or by prelabeling oligonucleotide primers with T_4 polynucleotide kinase and gamma-labeled ^{32}P-ATP and examining amplified products by autoradiography. Two short tandem repeat polymorphic markers, *D6Nds4* and *D6Mit3,* believed to flank the mutation and to lie approximately 13 cM apart, were used to genotype the first 1003 animals. Mice produced at later stages from these two matings were typed with closer flanking markers and fall into three additional bins (not shown; see legend of Fig. 1). The distal marker *D6Mit184* was used to type the remaining progeny. The proximal marker used for screening was changed as newer markers became available and as the position of these markers on our genetic map was determined (Dietrich et al. 1992). Therefore, the proximal markers used subsequently to *D6Nds4* in combination with *D6Mit184* were *D6Mit119* (mice 1004–1200), followed by *D6Mit240* (mice 1201–1222), and finally *D6Mit275* (mice 1223–1328). Mice carrying recombinations between the proximal and distal markers in each bin of animals were typed further with molecular markers to locate recombination breakpoints. Only 1329 of the 1383 mice were typed.

The murine *Evx1* gene is a homolog of the Drosophila *even-skipped* gene. *Evx1* was mapped near the *Hoxa* locus on mouse Chr 6 by recombinant inbred strain analysis (Dush and Martin 1992). The human EVX1 gene lies approximately 45 kb away from the HOXA13 (formerly *Hox-1.10*) gene (Faiella et al. 1991). Therefore, the murine homolog would be expected to lie adjacent to the *Hoxa* locus if there is conservation of the organization of genes in this region. The murine *Evx1* gene also is expressed in the developing limb bud and, thus, could be considered a candidate for the *Hd* locus. To test this hypothesis, we first wanted to verify its position on Chr 6 and performed RFLP analysis only with the mice carrying recombination breakpoints between the closely flanking markers *D6MIT119* and *D6MIT184* (15 mice). An *Evx1* genomic clone (pT2) was kindly provided by Mark Lewandoski and Gail Martin. We used a 2.5-kb *Sal*I genomic restriction fragment spanning the first and second exons of this gene to identify RFLPs. This probe was shown to be free of repetitive elements by genomic blot hybridization (data not shown). To find an RFLP for this gene between CASA/Rk, B6, and B6C3Fe, genomic DNA was digested with various restriction enzymes shown to have a high probability for revealing differences (Bowden et al. 1989). The genomic blots were probed with a ^{32}P-labeled (Feinberg and Vogelstein 1983) *Sal*I fragment encompassing the first exon, first intron, and second exon of the *Evx1* gene. Fragment sizes observed for *Sac*I and *Xba*I digests of this gene with this probe were ~13 kb each for CASA/Rk. B6 and B6C3Fe had fragments sizes of ~19 kb and 11 kb, respectively. In all 15 mice tested, no recombinations were ob-

Correspondence to: J.W. Innis

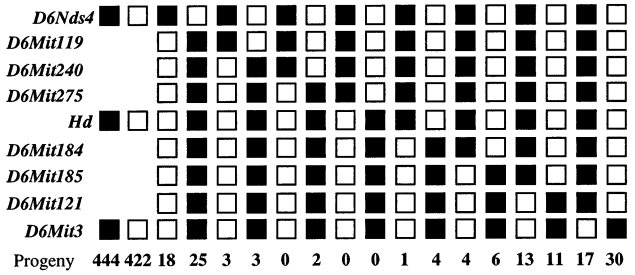

Fig. 1. Haplotype analysis. Backcross mice were divided into four bins (A–D) over the course of our studies defined by the two flanking markers used to type new backcross offspring. Bins B–D include 325 mice and are not shown; two recombinant chromosomes were identified in these bins, and the data are incorporated in Fig. 2. Gaps in the figure are left to indicate that only mice showing recombination within the interval defined by the markers used for the bin were typed further with all molecular markers shown. The number of progeny with each haplotype are indicated. No difference in the recombination frequency was observed between male or female meiosis (data not shown); therefore, male and female data are combined. **Black squares** refer to the B6C3Fe chromosomes, and **open squares** refer to the CASA/Rk chromosome. Some molecular markers were tested because of their reported position on the chromosome (Dietrich et al. 1992) and are not shown in Figs. 1 or 2 because they were found to lie proximal to *D6Mit240.* This list includes *D6Mit74, D6Mit42, D6Mit33, D6Mit142, D6Mit75, D6Mit43, D6Mit224,* and *D6Mit276.* These markers were not used for further typing after their general position was determined to be far from the mutation.

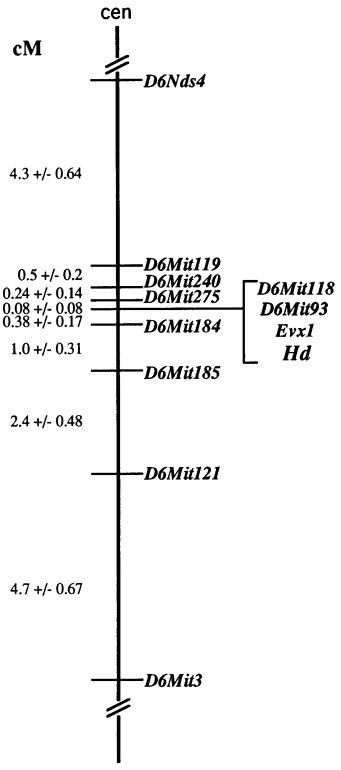

Fig. 2. Map of proximal mouse Chr 6. Genetic distances and standard deviations are shown. Markers *D6Mit118* and *D6Mit93,* and a RFLP within the *Evx1* gene could not be separated from the mutation. The data have been submitted to the Mouse Genome Database, accession number MGD-CREX-317.

served between the mutation, the nonrecombinant molecular markers *D6Mit118* and *D6Mit93,* and *Evx1.* These data place *Evx1* close to the *Hoxa* locus and make *Evx1* a candidate for *Hd.*

Figure 1 shows the haplotype analysis for the first bin of backcross progeny with the probes described above. The closest proximal flanking marker, *D6Mit275,* lies 0.08 ± 0.08 cM from *Hd.* The closest distal marker, *D6Mit184,* lies 0.38 ± 0.17 cM away. In addition to the *Evx1* gene, molecular markers *D6Mit118* and *D6Mit93* could not be separated from the mutation in this cross. *D6Mit93* lies within the 3′ untranslated region of the *Hoxa2* (formerly *Hox-1.11*) gene (Tan et al. 1992). The data do not allow us to position the mutation proximal or distal to the *Hoxa* locus nor to orient the *Hoxa* locus on the chromosome.

Figure 2 shows a summary of the genetic distances between loci mapped in this study. No significant differences were observed in the male versus female recombination frequencies (data not shown). The order and genetic distances between the markers in all of the mice were determined to be centromere –*D6Nds4*–4.3 cM–*D6Mit119*–0.5 cM–*D6Mit240*–0.24 cM–*D6Mit275*–0.08 cM–*Hd, D6Mit118, D6Mit93* (=*Hoxa2*), *Evx1*–0.38 cM–*D6Mit184*–1.0 cM–*D6Mit185*–2.4 cM–*D6Mit121*–4.7 cM–*D6Mit3.*

The closest flanking markers identified so far are *D6Mit275* (proximal) and *D6Mit184* (distal), which are separated from each other in our cross by 0.45 ± 0.18 cM. Three genetic markers could not be separated from the mutation in this backcross. These data place *Hd* closer to the *Hoxa* locus than shown before, establish close proximal and distal genetic markers between which the mutation must reside, and provide new information about the genetic distances between newer markers on the chromosome in this region.

One of the nonrecombinant markers, *D6Mit93,* lies within the *Hoxa2* gene. Previous work revealed recombination between a *Hoxa3* (formerly 1.5) RFLP and *Hd,* which placed the mutation 0.85 cM from the gene (Mock et al. 1987). The position of the mutation proximal or distal to the marker was not determined in that study; however, the data were more compatible with a proximal location for the mutation unless the mouse carrying the crossover was a double recombinant. If the *Hd* locus is proximal to *Hoxa3,* then knowledge of the orientation of the *Hoxa* cluster on the chromosome could be used to deduce whether other members of the *Hoxa* complex are candidates for *Hd.* Therefore, assessment of the genotype of this animal would prove extremely valuable given the data presented in our paper. Unfortunately, the sample from this single recombinant animal is no longer available (Beverly Mock, personal communication). In our cross, no recombination has yet been identified between *Hoxa2* and the mutation, suggesting that the recombinant mouse reported in the previous study is very rare. The lack of recombination between the mutation and *Hoxa2* in our cross could have resulted from 1) chance, if the mutation is, in fact, very close to *Hoxa2;* 2) recombination suppression due to the mutation; and/or 3) strain-related recombination preferences. Since the actual physical distance between recombination breakpoints is not known, it is not possible to conclude that suppression of recombination is occurring in the region around *Hd* in our cross. The issues of recombination suppression or strain-related preferences may be partially addressed by the analysis of recombination in a backcross utilizing *Mus spretus* (in progress). The genetic distances described in our map are consistent with other maps (Dietrich et al. 1992; Elliott and Moore 1993). However, this is the first study to present a high-resolution genetic map of the *Hd* locus relative to newer molecular markers and to define a genetic interval in which to focus research efforts to identify the mutation. Our study places *Hd* much closer to the *Hoxa* locus than previously shown and supports efforts to screen certain *Hoxa* genes and *Evx1* for the mutations.

Of the Hox genes known to be expressed in the limb, the patterns of 5′ *Hoxa* and *Hoxd* paralogs have been especially well described in the chick and the mouse (Dolle et al. 1991; Duboule 1991, 1992; Haack and Gruss 1993; Izpisua-Belmonte et al. 1991, 1992; Yokouchi et al. 1991). In contrast to *Hoxd* gene expression, which is coordinately restricted along the anterior/posterior (AP) axis, *Hoxa* expression patterns are restricted along the proximal/distal (PD) axis (Haack and Gruss 1993; Yokouchi et al. 1991).

For *Hoxa* genes, however, the PD restriction is established late. Both gene sets are initially activated in the posterior-distal aspect of the bud and spread anteriorly, but the expression of the *Hoxa* genes expands anteriorly across the entire AP axis, while that of *Hoxd* genes is restricted to posterior-distal regions. For *Hoxa* genes (*a10*, *a11*, and *a13*), expansion of the expression pattern proceeds along the periphery of the limb (Haack and Gruss 1993). The expression pattern of *Hoxa9* (formerly 1.7) has not been reported for the limbs. Rubin and associates (1987) reported a major *Hoxa9* transcript of 2.5 kb and minor transcripts of 1.9 and 3.9 kb in adult tissues and midgestation embryos. In embryos, the *Hoxa9* gene was expressed highly in the posterior spinal cord. Recently a targeted null allele of the *Hoxa10* gene was constructed in mice (Satokata et al. 1995). All male and female heterozygotes are fertile. Homozygous male and female mutants show full viability. *Hoxa10*-deficient males have bilateral cryptorchidism, and approximately 40% are sterile by the time they are 12 weeks of age, presumably because the normal shortening of the gubernacular cord and outgrowth of the gubernacular cord fail to occur. These structures are major sites of expression of *Hoxa10*. Approximately 80% of female mice deficient in *Hoxa10* are also sterile. Reproductive tissues and ovulation were normal; however, the lack of expression of *Hoxa10* in the distal oviduct and uterus leads to death of postimplantation embryos at day 2.5 to 3.5 p.c. Limb malformations were not described. A targeted null mutation of *Hoxa11* (formerly 1.9) was created in mice (Small and Potter 1993). Both heterozygotes and homozygotes for the null allele were viable and displayed skeletal malformations in the extremities and homeotic transformations of the axial skeleton. The thirteenth thoracic segment was found to be posteriorized to form an additional first lumbar vertebra, and the sacral region was anteriorized to generate another lumbar segment. The ulna and radius were malformed, the pisiform and triangular carpal bones were fused, and there was maldevelopment of the sesamoid in the forelimbs. In the hindlimbs, the tibia and fibula were inappropriately associated and misshapen at their distal ends. More recently, these mice have been shown to be infertile (Hsieh-Li et al. 1995). *Hoxa11* was shown to be expressed within the uterus, and the fact that homozygous null *Hoxa11* fetuses developed to term was interpreted to mean that the homozygous female is incapable of supporting pregnancy. A gene dosage effect was also observed in heterozygous mutant females in that severely reduced litter sizes were observed. Homozygous mutant males copulate normally but have a smaller and more coiled vas deferens and variable defects in spermatogenesis. Most males suffered from cryptorchidism. Mice heterozygous for the other targeted mutations described for the *Hoxa* genes at the 3′ end of the cluster do not show abnormalities like those for *Hoxa11*. Therefore, it appears that the level of expression, at least for *Hoxa11* and possibly for the other genes in the 5′ part of the *Hoxa* complex, may be a critical aspect of their biological effect, in contrast to genes in the 3′ end. Interestingly, significant antisense transcription from the *Hoxa11* locus was detected; cDNA probes specific for these transcripts detected expression within limbs of developing embryos by in situ hybridization (Hsieh-Li et al. 1995). The role that these putative genes play in limb development is not known although the expression of at least two was inferred to be disrupted by the *Hoxa11* targeted null mutation. Therefore, separation of the role of these genes in limb morphogenesis must await further experiments. On the basis of this discussion, genes in the 5′ end of the *Hoxa* cluster are excellent candidates for *Hd* because of the mutant phenotype and the expression patterns of the genes. It seems unlikely that *Hd* is a null mutation of *Hoxa10* or *Hoxa11*.

An RFLP within the *Evx1* gene was also not separable from the mutation in our cross. The position of *Evx1* in our cross is consistent with data using recombinant inbred strains (Dush and Martin 1992). The human EVX1 gene is located 45–50 kb away from the HOXA locus on the 5′ side of the cluster (Faiella et al. 1991). Given the highly conserved organization of the genes within the four vertebrate Hox clusters, it seems likely, given our genetic data, that the mouse gene resides in the same relative position. We are assembling a phage P1 contig spanning the nonrecombinant markers for the purpose of facilitating mutation screening and defining the *Hd* genetic interval in physical terms. One outcome of this work will be to determine the position of *Evx1* relative to the *Hoxa* complex in the mouse and to orient the complex on the chromosome. *Evx1* is expressed in the forelimbs on embryonic day 10.5 (Niswander and Martin 1993a, 1993b). It reaches a maximum level of expression on day 11.5, and expression ceases by 12.5 days. *Evx1* expression is located within the progress zone mesenchyme shortly after the formation of the apical ectodermal ridge primarily within the posterior-distal mesenchyme (Niswander and Martin 1993b). Recent work with targeted null mutations of *Evx1* show that homozygous embryos die early, failing to develop extraembryonic tissues or to form egg cylinders (Spyropoulos and Capecchi 1994). Interestingly, animals heterozygous for an *Evx1* null allele do not exhibit abnormal limb development. Therefore, it seems unlikely that *Hd* is simply a null allele of *Evx1*.

Most animals homozygous for *Hd* die in utero (Post and Innis, unpublished). The cause of death is unknown, and the temporal distribution of intrauterine deaths is not known. In our experience, lethality in monodactyls is not 100%. Examination of embryos and offspring of heterozygous matings reveals that all organs other than limbs appear normally formed except for occasional large cystic structures of the kidney and ureter (data not shown). All homozygous mutant embryos are generally smaller than their normal or heterozygous mutant littermates (L.C. Post, unpublished observations). We have been successful in generating eight liveborn homozygous animals. Liveborn homozygotes are reported to be infertile (Hummel 1970), and this is also true in our experience.

The complex cellular events that ultimately produce patterned, morphological development are poorly understood. Hypodactyly is an outstanding mutant to explore because of the failure of development of only the first digit in heterozygotes and digits one through four with more proximal skeletal defects in homozygotes. We propose that the normal product of the *Hd* gene is critical for early branching in the formation of the mammalian digital arch (Shubin and Alberch 1986). Considerable new information is likely to be gained through examination of the expression of genes such as sonic hedgehog (*Shh*), fibroblast growth factor 2 (*Fgf2*), fibroblast growth factor 4 (*Fgf4*), and bone morphogenetic protein 2 (*Bmp2*) in developing limbs of *Hd* homozygotes. In such expression studies, the markers that we have identified to be nonrecombinant with the *Hd* locus will allow embryo genotyping prior to the occurrence of limb malformation.

Acknowledgments. This work was supported by grants from the Phoenix Memorial Fund, the Rackham Graduate School of the University of Michigan, the Office of the Vice President for Research (University of Michigan), and a Junior Investigator Award from NICHD grant HD28820. J.W. Innis also acknowledges support from the Departments of Human Genetics and Pediatrics. The authors wish to thank Marion Buckwalter, David Burke, Margit Burmeister, Sally Camper, Jeff Chamberlain, Doug Mortlock, and Didi Robins for helpful suggestions and critical reading of the manuscript. We express our appreciation to Hope Sweet for providing unpublished information on the *Hd* strain. We thank Jian Shi for his help with the mouse colony and Sandy Jones and Lou Cubba for technical assistance.

References

Bowden, D., Muller-Kahle, H., Gravius, T., Helms, C., Watt-Morgan, D., Green, P., Donis-Keller, H. (1989). Identification and characterization of 23 RFLP loci by screening random cosmid genomic clones. Am. J. Hum. Genet. 44, 671–678.

Dietrich, W., Katz, H., Lincoln, S., Shin, H.-S., Friedman, J., Dracopoli,

N., Lander, E. (1992). A genetic map of the mouse suitable for typing intraspecific crosses. Genetics 131, 423–447.

Dolle, P., Izpisua-Belmonte, J.-C., Boncinelli, E., Duboule, D. (1991). The Hox-4.8 gene is localized at the 5′ extremity of the Hox-4 complex and is expressed in the most posterior parts of the body during development. Mech. Dev. 36, 3–13.

Duboule, D. (1991). Patterning in the vertebrate limb. Curr. Opin. Genet. Dev. 1, 211–216.

Duboule, D. (1992). The vertebrate limb: a model system to study the Hox/HOM gene network during development and evolution. BioEssays 14, 375–384.

Dush, M., Martin, G.R. (1992). Analysis of mouse Evx genes: *Evx-1* displays graded expression in the primitive streak. Dev. Biol. 151, 273–287.

Elliott, R., Moore, K.J. (1993). Mouse Chromosome 6. Mamm. Genome 5(Suppl.), S79–S103.

Faiella, A., D'Esposito, M., Rambaldi, M., Acampora, D., Balsofiore, S., Stornaiuolo, A., Mallamaci, A., Migliaccio, E., Gulisano, M., Simeone, A., Boncinelli, E. (1991). Isolation and mapping of EVX1, a human homeobox gene homologous to *even-skipped*, localized at the 5′ end of HOX1 locus on chromosome 7. Nucleic Acids Res. 19, 6541–6545.

Feinberg, A., Vogelstein, B. (1983). A technique for radiolabelling DNA restriction endonuclease fragments to high specific activity. Anal. Biochem. 132, 6–13.

Haack, H., Gruss, P. (1993). The establishment of murine Hox-1 expression domains during patterning of the limb. Dev. Biol. 157, 410–422.

Hsieh-Li, H., Witte, D., Weinstein, M., Branford, W., Li, H., Small, K., Potter, S. (1995). *Hoxa11* structure, extensive antisense transcription, and function in male and female fertility. Development 121, 1373–1385.

Hummel, K. (1970). Hypodactyly, a semidominant lethal mutation in mice. J. Hered. 61, 219–220.

Izpisua-Belmonte, J.C., Tickle, C., Dolle, P., Wolpert, L., Duboule, D. (1991). Expression of the homeobox Hox-4 genes and the specification of position in chick wing development. Nature 350, 585–589.

Izpisua-Belmonte, J.-C., Duboule, D. (1992). Homeobox genes and pattern formation in the vertebrate limb. Dev. Biol. 152, 26–36.

Miller, S., Dykes, D., Polesky, H. (1988). A simple salting out procedure for extracting DNA from human nucleated cells. Nucleic Acids Res. 16, 1215.

Mock, B., D'Hoostelaere, L., Matthai, R., Huppi, K. (1987). A mouse homeobox gene, *Hox*-1.5, and the morphological locus, *Hd*, map to within 1 cM on chromosome 6. Genetics 116, 607–612.

Niswander, L., Martin, G.R. (1993a). FGF-4 and BMP-2 have opposite effects on limb growth. Nature 361, 68–71.

Niswander, L., Martin, G.R. (1993b). FGF-4 regulates expression of *Evx1* in the developing mouse limb. Development 119, 287–294.

Rubin, M., King, W., Toth, L., Sawczuk, I., Levine, M., D'Eustachio, P., Nguyen-Huu, M.-C. (1987). Murine Hox-1.7 homeobox gene: cloning, chromosomal location and expression. Mol. Cell. Biol. 7, 3836–3841.

Satokata, I., Benson, G., Maas, R. (1995). Sexually dimorphic sterility phenotypes in *Hoxa10*-deficient mice. Nature 374, 460–463.

Scott, M. (1992). Vertebrate homeobox gene nomenclature. Cell 71, 551–553.

Shubin, N., Alberch, P. (1986). A morphogenetic approach to the origin and basic organization of the tetrapod limb. Evol. Biol. 20, 319–387.

Small, K., Potter, S. (1993). Homeotic transformations and limb defects in Hoxa-11 mutant mice. Genes Dev. 7, 2318–2328.

Spyropoulos, D., Capecchi, M. (1994). Targeted disruption of the *even-skipped* gene, *evx-1*, causes early postimplantation lethality of the mouse conceptus. Genes Dev. 8, 1949–1961.

Tan, D.-P., Ferrante, J., Nazarali, A., Shao, X., Kozak, C., Guo, V., Nirenberg, M. (1992). Murine *Hox-1.11* homeobox gene structure and expression. Proc. Natl. Acad. Sci. USA 89, 6280–6284.

Yokouchi, Y., Sasaki, H., Kuroiwa, A. (1991). Homeobox gene expression correlated with the bifurcation process of limb cartilage development. Nature 353, 443–446.